A reduced-order framework for performance mapping of compact parallel-channel evaporator

M. Pedroza-Torres [a], V. Dupont [b], R. Rioboo [c], A. Hernández [d], S. Gendebien [e] and V. Lemort [f]

[a] *Thermodynamics Laboratory / Université de Liège, Liège, Belgium, mptorres@uliege.be*
[b] *Calyos, Charleroi, Belgium, vincent.dupont@calyos-tm.com*
[c] *EHP, Nivelles, Belgium, rri@ehp.space*
[d] *Thermodynamics Laboratory / Université de Liège, Liège, Belgium, jahernandez@uliege.be*
[e] *Thermodynamics Laboratory / Université de Liège, Liège, Belgium, sgendebien@uliege.be*
[f] *Thermodynamics Laboratory / Université de Liège, Liège, Belgium, Vincent.Lemort@uliege.be*

Abstract:
The increasing demand for thermal management of electronic components in modern aerospace and terrestrial applications has driven the development of two-phase mechanically pumped loops (2PMPLs), equipped with compact evaporators capable of exploiting the latent heat of vaporisation to manage high heat-flux operating conditions. Among heat acquisition components, compact parallel-channel evaporators are particularly attractive due to their high wetted-area-to-volume ratio; however, their integration into system-level models remains challenging because of the lack of reliable constitutive equations for the fluid-side heat transfer coefficient (HTC) in such non-standard geometries. This work proposes a reduced-order framework for obtaining an effective HTC capable of quantifying the average heat transfer performance of the evaporator at a given operating point. Wall temperature measurements, obtained under controlled heat input conditions, are combined with finite element modelling to infer fluid-side HTC values through an inverse heat transfer approach. The estimations, performed on cross-sections associated with six control points distributed along the axial length of the evaporator, enable the determination of an average heat transfer value for the component, interpreted as an effective HTC representative of its behaviour under the corresponding steady-state operating condition. The effective values obtained for the heat transfer coefficient and the internal wall temperature are subsequently employed in a consistency analysis using a one-dimensional thermo-hydraulic model of a two-phase mechanically pumped loop. This procedure ensures that the reduction of the heat transfer phenomenon to a single effective value remains compatible with the expected enthalpy evolution and the overall system response. The proposed reduced-order methodology aims to provide a consistent basis for the performance analysis of parallel-channel evaporators and to support design-oriented studies of two-phase thermal management systems.

Keywords:
Conductivity analysis; Effective HTC; Inverse heat transfer; Reduced-order modelling; Two-phase.

1. Introduction

In modern technological applications, the intensive use of energy within electronic equipment presents the current challenge of conceiving and operating thermal management architectures capable of ensuring appropriate operating conditions. This is particularly true in the aerospace sector, where the demands for compactness, reliability, and high performance have driven, since the second half of the twentieth century, research into cooling technologies based on phase-change phenomena, among which the two-phase mechanically pumped loop architecture can be found [1]. This technology is not limited to aerospace applications, but also offers strong potential for deployment in terrestrial systems, where growing thermal management demands from high heat flux devices (>10 W/cm^2) call for solutions specifically designed to acquire, transport, and reject large heat loads in compact and difficult-to-access operating environments [2]

The basic operating logic of the 2PMPL can be summarised through the concept of heat transport by means of a thermal bus [3], in which a diabatic section (heat acquisition zone) absorbs energy losses from a given process and transfers it to a working fluid responsible for transporting and releasing it at another location

specifically intended for heat rejection. In contrast with the simplicity of this concept, the details associated with component and system design present technical and research challenges that continue to engage the heat transfer and applied thermodynamics community to this day [4].

Once the application context has been established, the present work focuses the discussion on the technical challenge of designing an efficient heat acquisition zone, for which the compact parallel-channel evaporator typology has been selected as a case study. In this regard, a wide range of geometric, material, structural, and operational parameters could be considered [5]; However, the integration of data related to the heat transfer capability of a component within the main loop requires a robust quantification of the heat transfer coefficients governing the interaction between the internal evaporator walls and the working fluid. To this end, numerous laboratories have undertaken the quantification of these coefficients for a broad range of fluids and hydraulic diameters [6]. Nevertheless, for less standard geometries and parallel-channel configurations, the available correlations often present a very narrow range of applicability or are simply non-existent [4].

The present work therefore proposes a reduced-order methodology for obtaining effective HTC values through the inference of these coefficients based on the solution of an inverse heat transfer problem, making use of conductive analysis of the 2D temperature field in evaporator cross-sections, real measurements obtained from a two-phase loop adapted for operation with acetone, together with thermodynamic consistency verification through a one-dimensional thermo-hydraulic model of the loop. These effective HTC values are plotted against different operating parameters in order to comparatively analyse the behaviour of the steady-state operating points. Finally, the evolution of the effective HTC as a function of vapour quality and volumetric flow rate is proposed as an example of a performance map with the potential to be employed as a tool for operating point selection, based on the criterion of maximising the heat transfer index for the particular evaporator geometry under analysis.

2. The two-phase mechanically pumped loop testbench

2.1. System-level: The loop

For the purpose of characterising the operation of parallel-channel evaporators, the capillary jet loop developed by Calyos [7], was adapted through the addition of a pumping stage. Figure 1a shows the experimental set-up of the acetone pumped loop, while the schematic in Figure 1b highlights its main components and the most relevant sensors for the present experimental campaign.

a)

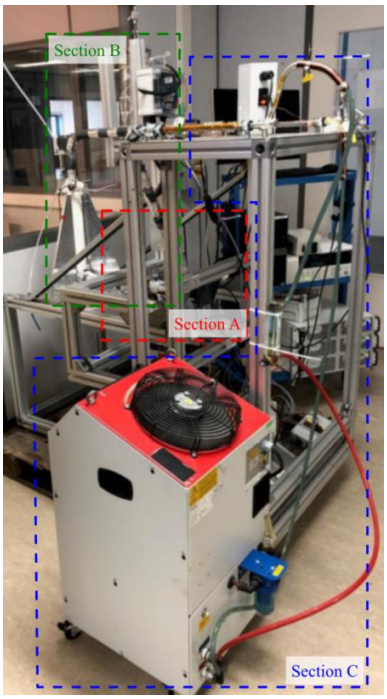

b)

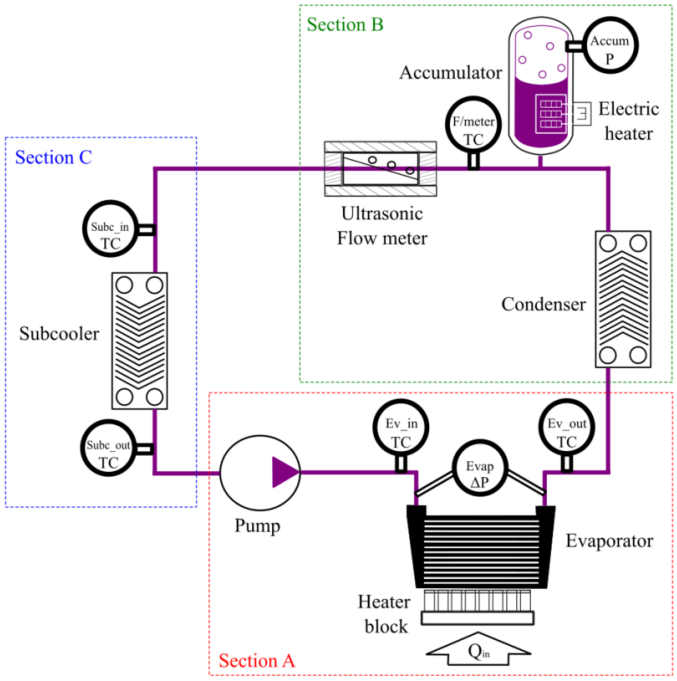

Figure. 1. *Mechanically pumped loop: a) Calyos testbench, b) Diagram of the main components*

In this context, the basic operation of the 2PMPL can be summarised in three sequential stages: (i) Heat acquisition: this process begins in the evaporator, where heat transfer from the hot source drives the phase change of the confined working fluid under near-isothermal conditions; (ii) Heat transport: fluid circulation is

ensured by the pump, while saturation conditions are actively controlled through the regulation of pressure (and temperature) by the accumulator, which is equipped with an electric heater; (iii) Heat rejection: finally, the condenser (and subcooler) release heat to the cold sink, returning the fluid to the liquid state and ensuring continuity of single-phase pumping.

2.2. Component level: The evaporator

A parallel-channel configuration was selected for the diabatic heat acquisition component in this experimental campaign. The evaporator named Macro_2_7 consisting of 12 identical rectangular channels with cross-sectional dimensions of 2.7 mm × 3.2 mm and a length of 57 mm, manufactured by selective laser sintering using AlSi10Mg aluminium alloy, with an average thermal conductivity of 117.57 W/m·K. Regarding the instrumentation required for estimation of the effective heat transfer coefficient, Figure 2 shows the axial distribution of the measurement points (P1 to P6) located at the contact interface between the heating block and the region dedicated to heat transfer, the employed instrumentation consists of T-type thermocouples embedded through grooves machined into the external surface of the evaporator (maximum depth of 0.7 mm) and distributed longitudinally along the flow direction.

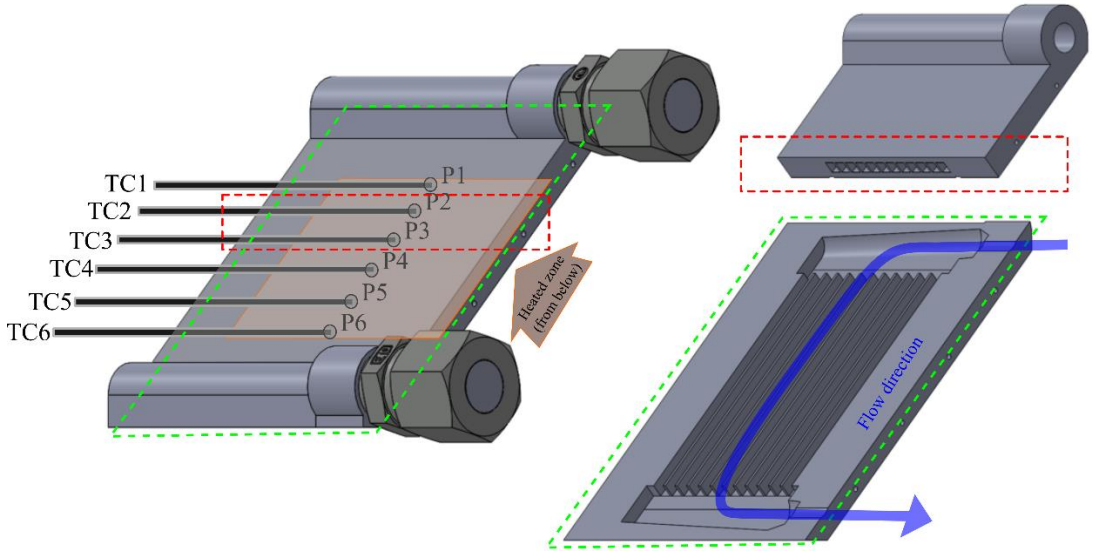

Figure. 2. *External measurement points on the evaporator and sectional views*

With regard to the internal channel arrangement, Figure 3 details the main dimensions and geometric descriptors of the tested evaporator, such as aspect ratio and hydraulic diameter, together with a qualitative representation of the temperature evolution shown by isothermal lines resulting from bottom heating during the finite element conductive analysis.

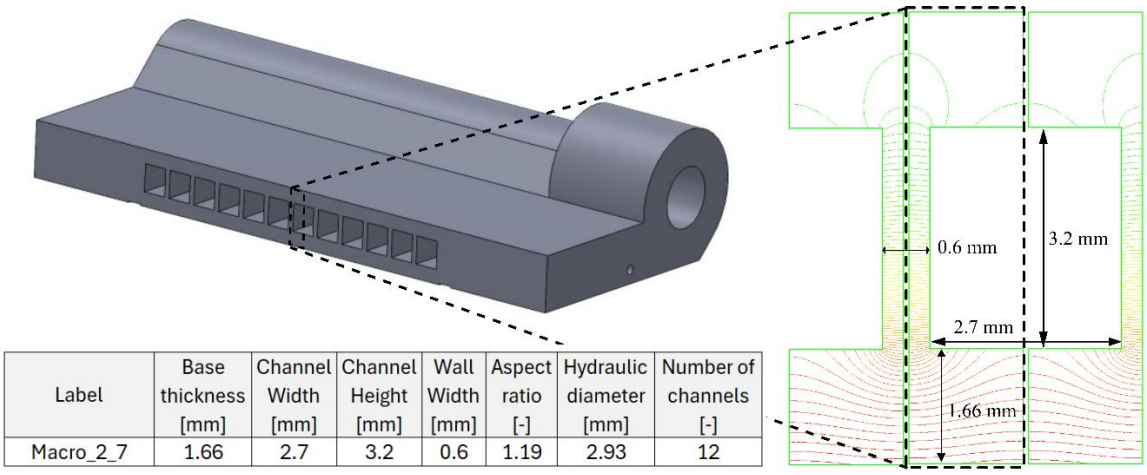

Label	Base thickness [mm]	Channel Width [mm]	Channel Height [mm]	Wall Width [mm]	Aspect ratio [-]	Hydraulic diameter [mm]	Number of channels [-]
Macro_2_7	1.66	2.7	3.2	0.6	1.19	2.93	12

Figure. 3. Dimensions for conductivity analysis on parallel channel evaporator

2.3. Data set

Based on the technical equipment described in the previous paragraphs and the selection of acetone as the working fluid, Table 1 presents 19 steady-state operating points to assess the relevance of the effective heat transfer coefficient definition proposed in the present work.

Table 1. *Steady-state data points from the Macro_2_7 evaporator operating with acetone*

SS ID	P_{acc}, bar	T_{subc}, °C	VFR, l/min	Q_{in}, W	ΔP_{evap}, kPa	$T_{wall,ext,avg}$, °C
1	2.16	60.2	2.13	194.5	15.1	39.3
2	2.16	58.4	2.16	581.5	15.4	78.7
3	2.16	57.7	2.18	773.3	15.4	97.4
4	0.40	11.4	1.39	194.3	6.2	52.4
5	0.38	10.1	1.40	242.5	6.2	60.7
6	0.37	9.1	1.40	290.6	6.6	68.9
7	0.38	9.3	1.40	338.6	6.3	77.4
8	0.38	9.3	1.40	386.5	6.6	86.2
9	0.37	9.4	1.42	194.1	6.5	44.6
10	0.37	8.4	1.44	580.0	6.4	93.8
11	0.45	13.3	0.75	580.6	6.9	62.8
12	0.57	18.4	1.36	775.1	8.1	70.7
13	0.57	18.4	0.75	775.1	8.2	71.0
14	0.47	10.6	0.72	200.3	1.6	63.4
15	0.47	10.1	0.71	225.2	1.6	69.1
16	0.47	10.2	0.71	250.1	1.6	74.0
17	0.48	10.2	0.71	274.9	1.6	78.8
18	0.48	10.3	0.72	299.6	1.6	82.9
19	0.47	9.8	0.64	323.2	1.6	86.7

It is important to note that these experimental points were originally defined using subcooling, volumetric flow rate, and inlet power levels focused on reproducing outlet vapour quality conditions equal to zero. Although they do not represent archetypal optimal operating points for a phase-change heat acquisition system, they are regarded as a data set capable of providing a solid basis to assess the qualitative behaviour of the effective heat transfer coefficient after mapping the evolution of its magnitude in coordinate systems based on operating variables.

3. A reduced-order modelling framework

3.1. The inverse heat transfer problem

The inverse heat transfer problem is defined as the mathematical and computational task of working backwards to determine unknown thermal causes (such as coefficients representative of heat transfer capability) from known thermal effects (such as temperature measurements). In this sense, from the fluid perspective, the heat transfer coefficient, according to its fundamental definition, is presented in Equation (1):

$$h = \frac{q}{T_{wall} - T_{fluid}} \tag{1}$$

where h is interpreted as a proportionality constant between the heat flux q and the temperature difference required to sustain the existence of such heat transfer. Although the heat flux may be estimated from imposed experimental conditions together with an appropriate evaluation of heat losses, determining the fluid temperature evolution within the diabatic component—and, more importantly, the wall temperature evolution at the solid–liquid interface—requires dedicated instrumentation which, even under highly controlled conditions, may yield heat transfer coefficient values with wide uncertainty ranges, particularly under operating regimes involving phase-change phenomena. In this context, the inverse heat transfer problem offers a computational approach to this challenge by defining, in this case, a numerical boundary condition for the heat transfer coefficient representative of the fluid heat acquisition capability, whether associated with the convective characteristics of the flow regime or the possible onset of nucleation. The method then verifies whether, after imposing the theoretically transferred heat flux from the hot source, the resulting temperature field within the solid component reproduces the values measured by the available sensors. This iterative approach benefits from the numerical accuracy associated with the finite element method and the computational efficiency provided by tools such as FreeFEM++ [8], which was the platform selected for the present study.

3.2. Why a reduced-order approach?

Within the inherent complexity associated with modelling the thermodynamic evolution of systems and processes involving two-phase flow under diabatic conditions, the present work proposes a reduced-order formulation of the problem, understood as a physically structured low-dimensional thermo-hydraulic representation capable of preserving the dominant system-level behaviour, whose five main modelling assumptions are detailed in Table 2.

Table 2. *Assumptions for the reduced-order approach*

Conceptual Domain or practical constraint	Modelling assumption	Reduced-order representation strategy
Flow maldistribution in parallel-channel evaporators * Non-uniform flow distribution between channels * Uneven thermal loading between channels * Manufacturing-induced geometric variability	**1**	**Hypothesis of uniformity and axial representativeness** * The diabatic component is represented using an equivalent axial thermohydraulic 1D description assuming that dominant system-level behaviour can be approximated through conductive analysis and temperature measurements performed on the central channel of the evaporator under the assumption of a uniform heat load profile.
Two-phase flow representation * Local phase distributions and spatially heterogeneous void fraction * Interfacial momentum exchange and flow regime transitions * Local dryout and rewetting phenomena	**2**	**Homogeneous equilibrium model** * Liquid and vapour phases are represented using equivalent bulk thermodynamic states under local equilibrium assumptions, avoiding explicit resolution of interfacial topology and regime-dependent structures.
Constitutive equations for pressure drop in flow boiling * Lack of geometry-specific pressure drop correlations * Strong dependence on local flow structure * Uncertainty in two-phase friction mechanisms	**3**	**Experimentally constrained friction closure** * Pressure evolution is obtained from momentum conservation through a friction factor constrained by the differential pressure value between the evaporator outlet and inlet reported by the experimental measurements.
Heat transfer performance under single-phase and two-phase flow conditions * Absence of validated HTC correlations for specific geometries * Spatially varying boiling intensity * Geometry, fluid and pattern dependent heat-transfer mechanisms	**4**	**Effective Heat transfer coefficient (HTC)** * The heat transfer behaviour is represented through a single effective HTC value that must satisfy two conditions: (1) ensure an energy transfer equivalent to that experimentally reported in the diabatic zone, within a prescribed relative error margin; and (2) lead to an enthalpy evolution and thermodynamic variable profiles within the one-dimensional model that remain compatible with the system-level instrumentation data, within mean absolute error margin.
Limited sensor availability * Limited spatial observability * Inaccessibility of internal flow variables * Industrial instrumentation limitations	**5**	**Semi-empirical model for steady-state analysis** * System states and constitutive behaviour are reconstructed through conservation-based steady-state inference using sparse macro-scale measurements and physically constrained closure assumptions.

3.3. Workflow for effective HTC determination

Based on the modelling assumptions introduced in Section 3.2 and the inverse heat transfer problem task presented in Section 3.1, Figure 4 details the proposed workflow for obtaining effective HTC values from the available instrumentation data corresponding to each steady-state scenario reported in the data set (Table 2). The description of the workflow may begin from the input parameters required by the one-dimensional thermo-hydraulic processing block (*1D inner solver*) correspond to the list of experimentally measured values, including: pressure drop across the evaporator (ΔP_{evap}), volumetric flow rate within the loop (VFR), saturation pressure imposed by the accumulator (P_{acc}), and evaporator inlet temperature ($T_{in,evap}$). At this point, the *1D inner solver* is introduced as the computational structure responsible for adapting the evolution of the thermodynamic variables to the energy transfer conditions imposed within the diabatic zone, either by taking as input a predefined heat load profile (heat load mode) or by calculating it from a prescribed heat transfer coefficient (HTC mode). Returning to the upper-central region of Figure 4, the experimentally applied electrical power is employed as the input variable for calculating the energy theoretically transferred to the fluid after accounting for environmental heat losses. This transferred energy may be modelled as a power allocation profile per unit length (units in W/m). The specific shape of this profile depends on the heat transfer conditions associated with each steady-state operating scenario and is therefore unknown a priori for the particular evaporator geometry under analysis. It is at this stage that the reduced-order methodology introduces its first modelling assumption by considering a constant heat load profile per unit length within the diabatic zone. Subsequently, the *1D inner solver* is employed to obtain the estimated fluid temperature profile between the evaporator inlet and outlet.

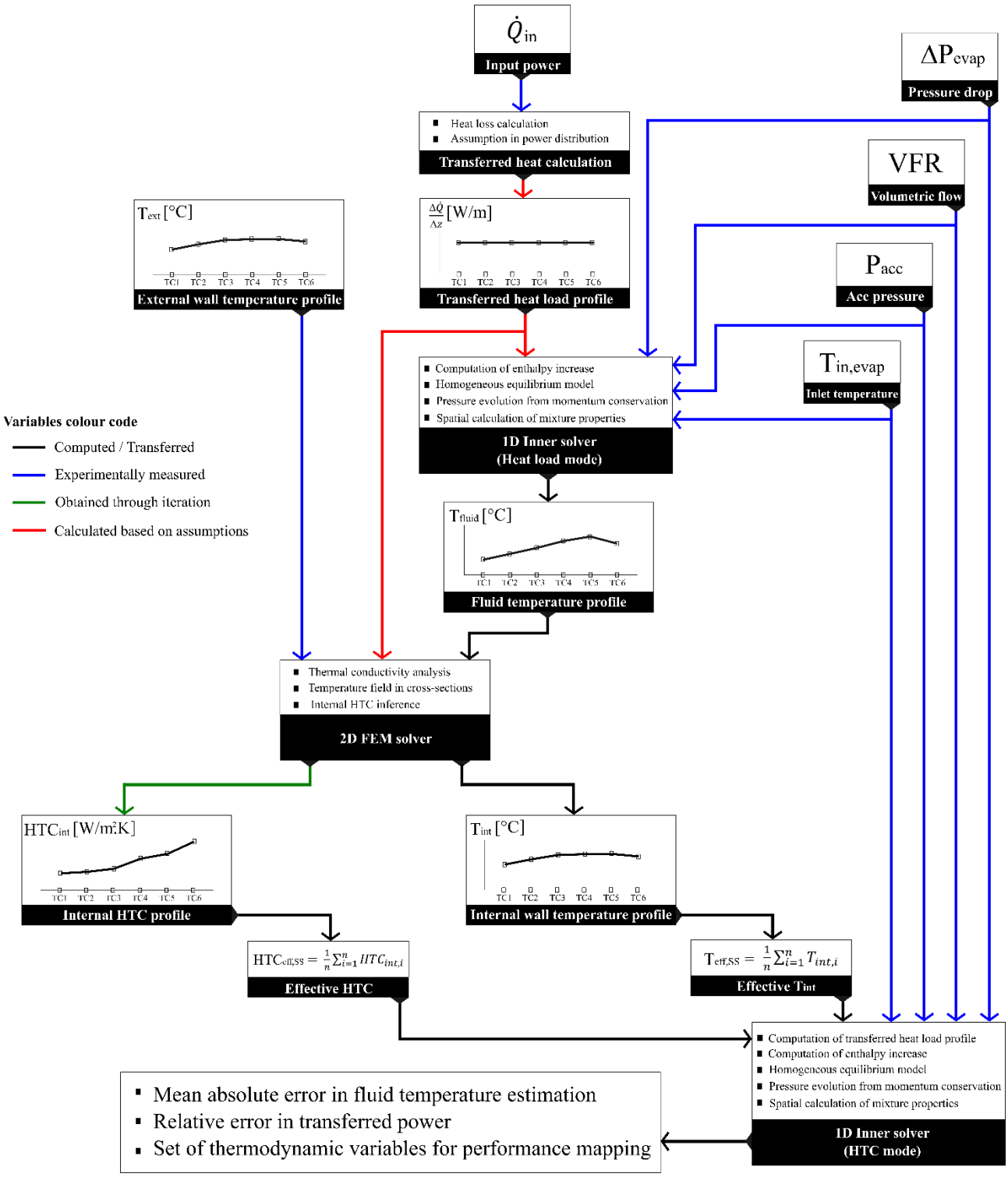

Figure. 4. *Workflow for effective HTC determination at each steady-state operating point*

The external wall temperature of the central channel, the uniform thermal load profile and the fluid temperature obtained from the *1D Inner solver*, are all introduced as input parameters to the block denoted as *2D FEM solver*, responsible for computing the conductive analysis of the transverse cross-sections corresponding to each measurement point (available thermocouple). Under the assumptions of thermal symmetry and limited flow maldistribution, half of the central channel (C-shaped profile) was selected as the representative element for the heat transfer dynamics and temperature field evolution in this reduced-order approach. Accordingly, the computational domain and its associated boundary conditions are detailed in Figure 5. Constant heat flux conditions are imposed at the lower boundary of the channel, zero-flux conditions are prescribed at the lateral boundaries due to thermal symmetry, and at the upper boundary due to insulation. A Robin-type boundary

condition, interpreted as a constant HTC condition, is introduced to encapsulate the complex interplay between convection and phase-change phenomena.

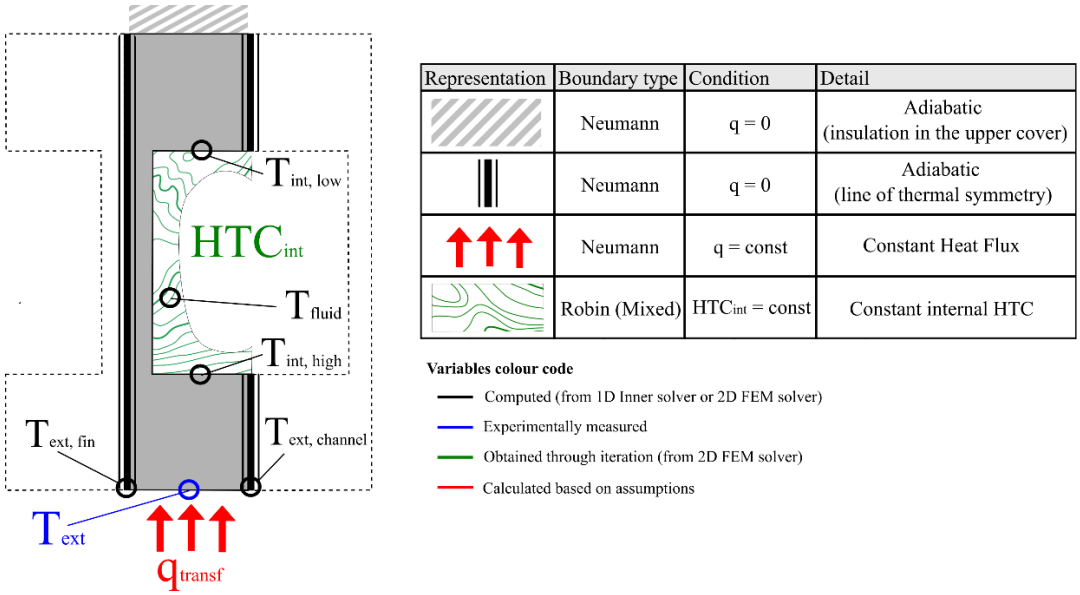

Figure. 5. *Boundary conditions for half-channel FEM calculation*

The logical sequence employed for the estimation of the internal heat transfer coefficients as well as the mean internal temperature within the cross-section of the central evaporator channel is presented in Figure 6.

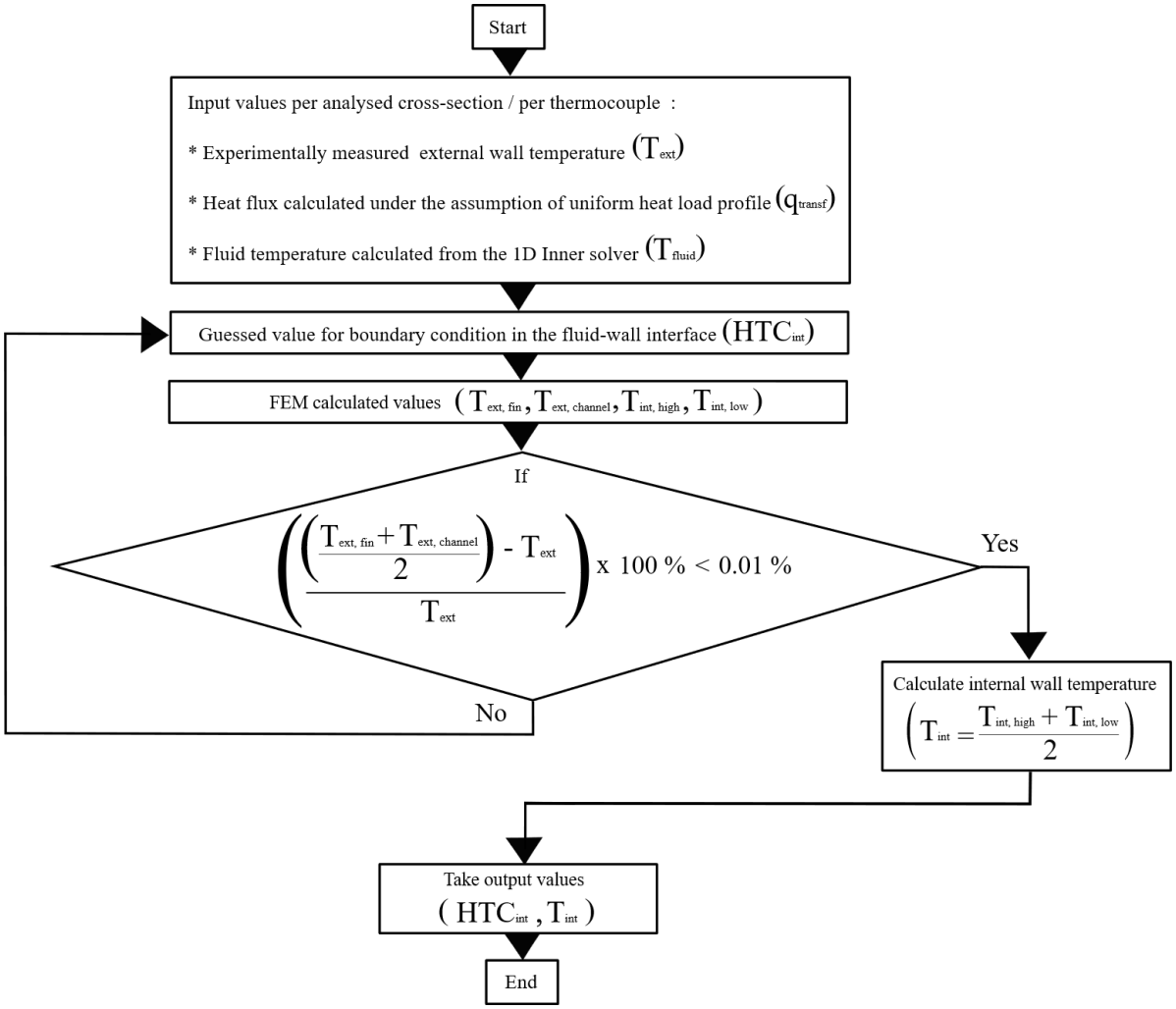

Figure. 6. *Flow diagram of the 2D FEM solver*

The required input values comprise: (i) the heat flux transferred to the fluid, q_{transf}, obtained from the calculation of the incoming electrical power, environmental heat losses, and the geometric surface associated with heat transfer; (ii) the fluid temperature inside the evaporator, T_{fluid}, extracted from the axial temperature evolution profile calculated under the assumption of homogeneous energy directly transfer to the fluid, where the total heat transfer rate is divided by the evaporator length (diabatic zone) to establish a constant heat load profile (units in W/m); and (iii) the external temperature, T_{ext}, measured by the thermocouple installed on the central channel. Starting from a representative guess value for the internal heat transfer coefficient, HTC_{int}, the imposed input conditions define the evolution of the 2D temperature field within the cross-section. A closure criterion is then established such that the average of the external temperatures at the fin center, T_{fin}, and at the channel center, T_{channel}, numerically matches the external temperature measured by the thermocouple, T_{ext}. As the final result of this iterative process, a value of HTC_{int} consistent with the measurements obtained from the experimental test bench is determined. Additionally, during the final iteration step, the wall temperatures at the midpoints of the upper and lower internal horizontal segments of the C-shaped profile, $T_{\mathrm{int,high}}$ and $T_{\mathrm{int,low}}$, are taken as reference values for the calculation of a representative internal channel temperature, whose average is defined as T_{int}.

This analysis scenario is repeated six times for each steady-state operating condition, since data from six thermocouples axially distributed between the heating surface and the evaporator are available (as shown in Figure 2), thereby enabling the determination of a single average value for the heat transfer coefficient. Such an average coefficient may therefore be regarded as an effective value capable of representing the internal evaporator conditions for the steady-state operating point under analysis, and will hereafter be referred to as $HTC_{eff,SS}$ whose formal definition is presented in Equation (2):

$$HTC_{eff,SS} = \frac{1}{n}\sum_{i=1}^{n} HTC_{int,i} \tag{2}$$

Where n represents the number of thermocouples (control points / analysed evaporator cross-sections), and HTC_{int} corresponds to the value obtained from the inverse heat transfer problem at each control point. Analogously, Equation (3) presents the definition of the effective temperature $T_{eff,SS}$ as the average of the internal temperatures of the wall:

$$T_{eff,SS} = \frac{1}{n}\sum_{i=1}^{n} T_{int,i} \tag{3}$$

These values are subsequently subjected to a thermodynamic consistency analysis using the one-dimensional model of a two-phase mechanically pumped loop described in the following section.

3.4. The thermo-hydraulic model (1D Inner solver)

Based on the model proposed by Sunada et al. in 2016 [3] for the longitudinal discretisation of a 2PMPL in a single-loop configuration, a system-level model has been developed capable of sequentially tracking the evolution of pressure, temperature, and vapour quality along the number of z cells defined for the spatial discretisation of the simulation scenario. It is at this stage that the effective values are assessed through the calculation of the power allocation per cell j within the diabatic zone, as detailed in Equation (4):

$$\left(\frac{\Delta\dot{Q}}{\Delta z}\right)_j = HTC_{eff,SS} * \beta_{wetted,j}(T_{eff,SS} - T_{fluid,j-1})\ ;\ j \in \mathcal{S} \tag{4}$$

Where $\Delta\dot{Q}$ represents a finite amount of transferred energy over a length Δz defined for each computational cell; $\beta_{wetted,j}$ represents the total wetted perimeter grouping all evaporator channels and arranged transversally with respect to the current cell j. $T_{fluid,j-1}$ represents the fluid temperature calculated in the immediately preceding cell and, under the assumption of sufficiently small computational cell sizes, is incorporated here as an adequate estimator of the fluid temperature in the current cell. Finally, $\mathcal{S}$ denotes the subset of diabatic cells over which the progression of the index j is defined.

For the purpose of quantifying the agreement between the thermodynamic profiles obtained from the effective heat transfer coefficients and the experimental measurements, two tolerance values were employed. The first, ε_{MAE}, is defined as the maximum admissible Mean Absolute Error (MAE) between the calculated property and the sensors distributed throughout the test bench. The second, ε_{transf}, establishes the maximum admissible percentage relative error for transferred power.

Figure 7 illustrates the thermodynamic consistency verification for the effective values calculated for steady-state scenario ID:13 with an MAE value of 0.6 °C in the estimation of the fluid temperature profile, and a percentage relative error of 2.67% in the transferred power, highlighting how the cell-wise power allocation enables the determination of a fluid temperature profile compatible with the data measured by the

instrumentation installed on the experimental test bench. This verification was applied to all effective HTC values calculated for the 19 steady-state scenarios reported in the data set, employing the tolerance criteria $\mathcal{E}_{MAE} = 1\,°C$ and $\mathcal{E}_{transf} = 7\%$.

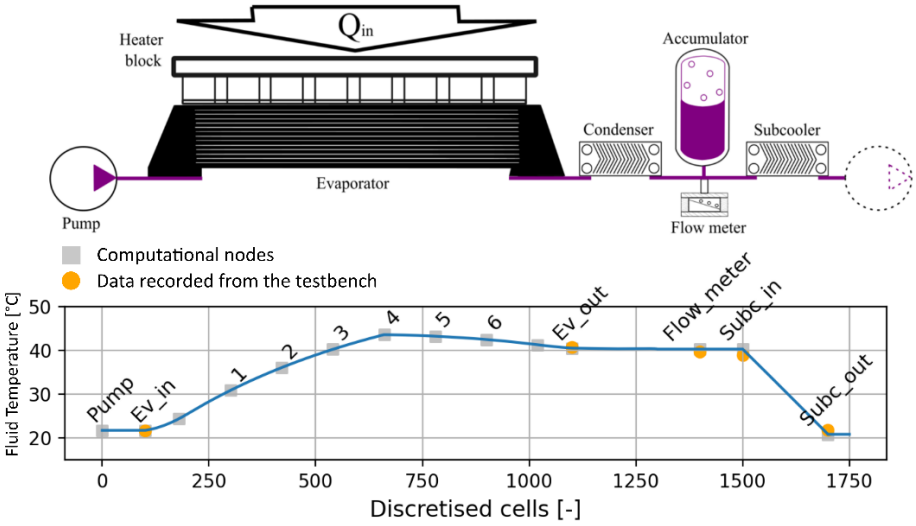

Figure. 7. *Verification of thermodynamic consistency of effective values in the 1D model (SS ID 13)*

At this stage, it is important to clarify that the thermo-hydraulic model is also employed in the present work as a calculation tool for the outlet quality of the evaporator under the steady-state conditions defined for each experimental point. Should further interest arise, the modelling assumptions, geometric parametrisation, and mathematical formulation of the 1D model are described in greater detail in other publications [9].

4. Effective HTC as a performance metric

The comparative performance of the evaporator, in terms of $HTC_{eff,SS}$ calculated for the 19 data points, is presented in Figure 8.

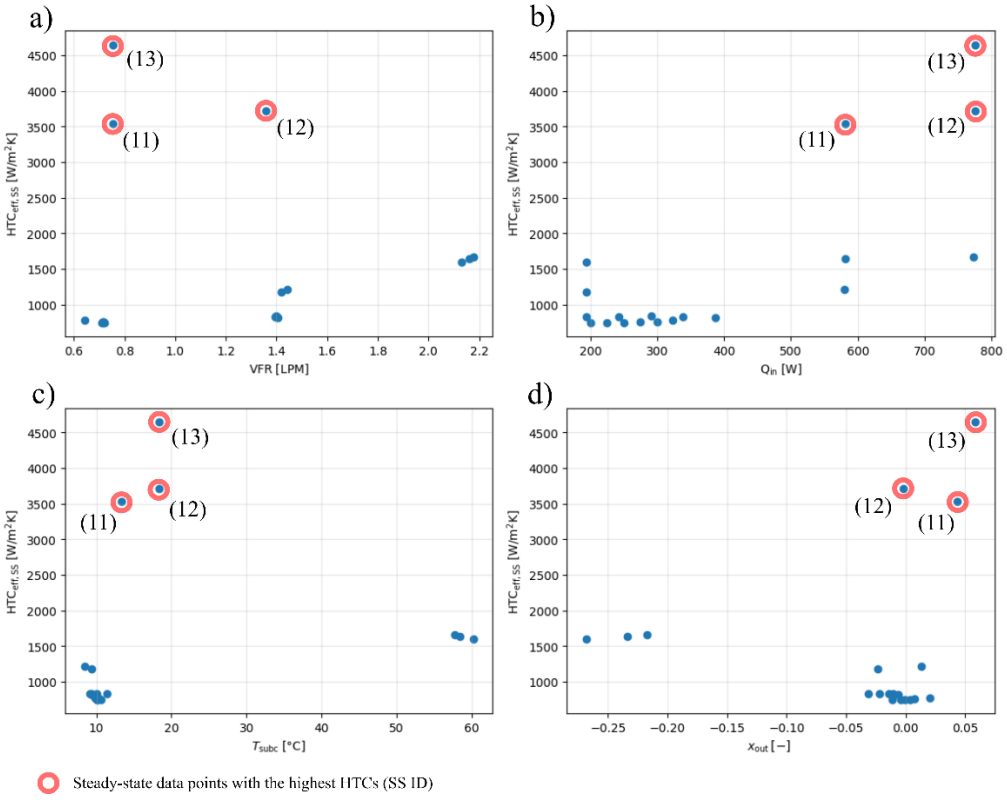

Figure. 8. *Comparative analysis of steady state data points in terms of $HTC_{eff,SS}$ against: a) volumetric flow rate, b) input power, c) subcooling temperature, and d) outlet vapour quality*

The heat transfer capability of points 11, 12, and 13 is particularly notable, which may be primarily explained by the phase change promoted by the operating conditions and input power levels associated with these points. In this regard, the quantitative comparison of the effective HTC obtained through the present reduced-order methodology is proposed as an indirect alternative for the identification of phase-change conditions.

Moving to the global performance map of the evaporator, Figure 9 shows the selected coordinate axes: volumetric flow rate (as the operating variable) and outlet vapour quality (as a representative parameter of the energetic state), onto which the progression of $HTC_{eff,SS}$ is mapped through interpolation of the values associated with each data point. It is of particular interest to note the presence of the two main mechanisms associated with HTC enhancement: (a) increased heat transfer linked to higher flow velocities (the convective contribution to heat transfer), and (b) increased heat transfer associated with phase change (nucleation / bubble formation). The presence of unexpectedly low or high HTC values at the threshold of phase change (outlet vapour quality equal to zero) is considered a subject for further investigation, as it may be related either to errors in the estimation of the power effectively transferred to the fluid or to the possible onset of boiling. Despite this, it is considered important to highlight the physical consistency that this reduced-order methodology can provide when discussing the best operating points within exploratory campaigns involving new parallel-channel evaporator architectures.

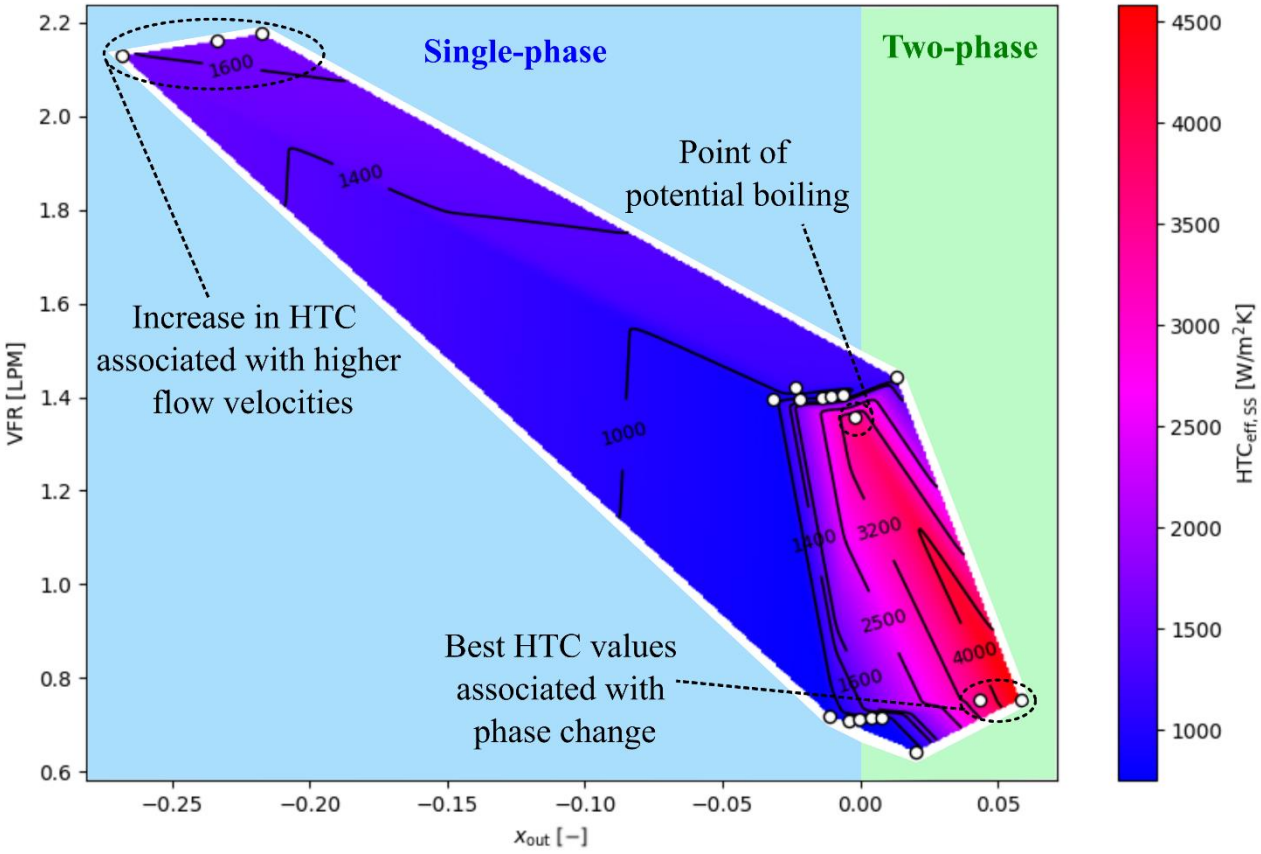

Figure. 9. *Evaporator performance map: Evolution of the effective HTC as a function of outlet vapour quality and volumetric flow rate*

5. Summary of the reduced-order methodology

The reduced-order methodology proposed in the present work is summarised in Figure 10.

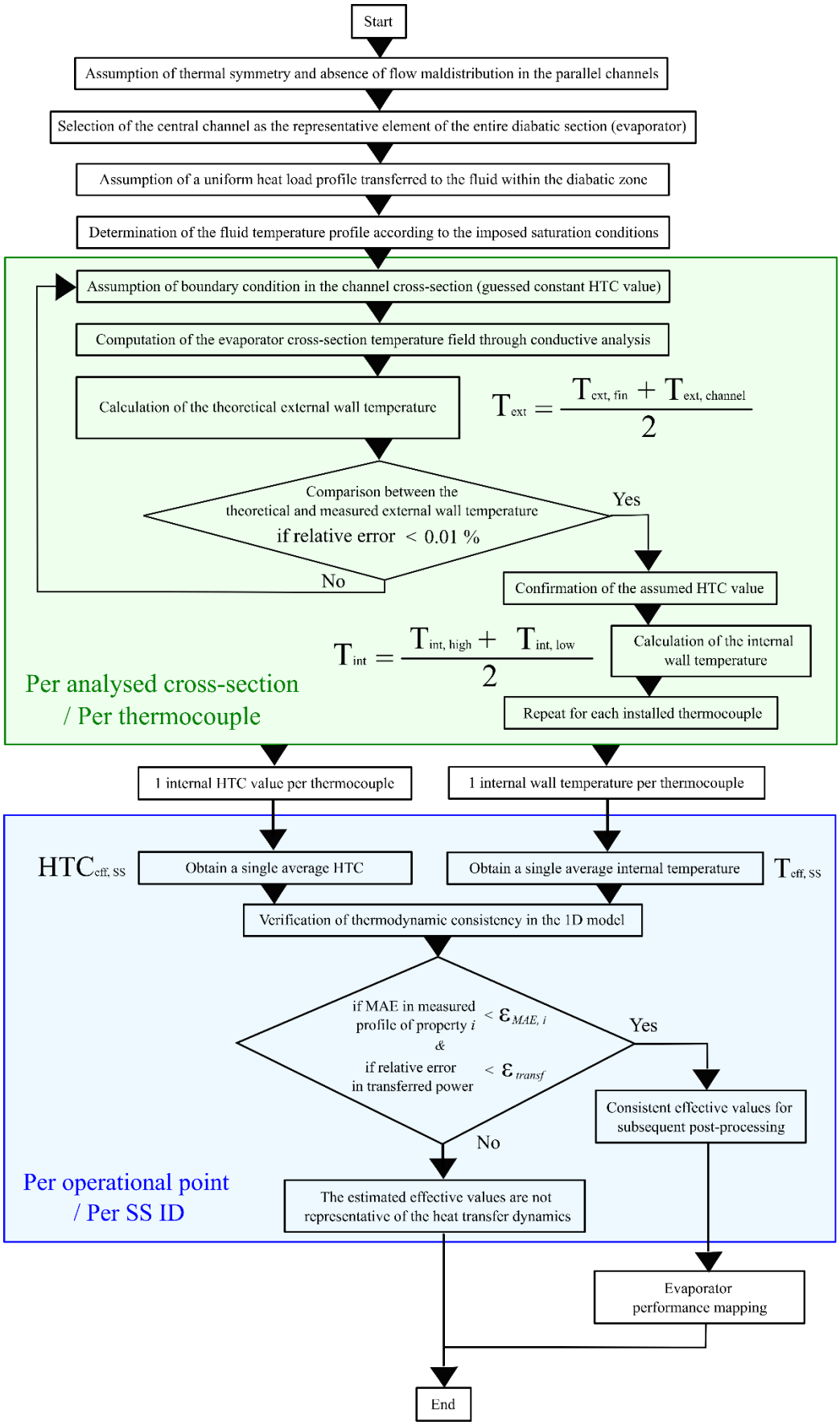

Figure. 10. *Flow diagram of the reduced-order methodology*

6. Conclusions and future work

- The proposed reduced-order framework demonstrated that effective HTC values obtained from inverse conductive analysis can reproduce experimentally measured system-level thermodynamic behaviour within prescribed tolerance margins.
- The methodology enables the transformation of sparse experimental measurements into operational performance maps as a tool to select operating conditions that maximize heat transfer performance.
- The obtained $HTC_{eff,SS}$ maps preserved physically meaningful trends associated with both convective enhancement at higher flow rates and heat-transfer intensification linked to phase-change conditions.
- The abstraction of $HTC_{eff,SS}$ maps into general-purpose functions has the potential to be implemented for the simulation of two-phase loop architectures at system level.
- The extension of these maps to a wider range of operating scenarios and evaporator geometries is envisaged in the near future.

Acknowledgments

This work has been made possible thanks to the MPL2030 project (Convention n° 8941 Skywin – AAP39), a result of the collaboration between the Walloon government, the Skywin competitiveness cluster, the industrial partnership of EHP-Calyos, and the academic collaboration between the University of Louvain and the University of Liège.

References

[1] Lv, Y. G. et al., “Review on thermal management technologies for electronics in spacecraft environment,” Energy Storage and Saving, vol. 3, p. 153–189, 2024.

[2] Es, J. v., and Gerner, H. J. Benefits and Drawbacks of Using Two-Phase Cooling Technologies in Military Platforms. Tech. rep., National Aerospace Laboratory NLR. 2011.

[3] Sunada, E. et al., “A Two-Phase Mechanically Pumped Fluid Loop for Thermal Control of Deep Space Science Missions,” in 46th International Conference on Environmental Systems, 2016.

[4] Cheng, L; Xia, G. High Heat Flux Cooling Technologies Using Microchannel Evaporators: Fundamentals and Challenges. Heat Transfer Engineering , Vol. 44, No. 16–18. p. 1470-1497. 2022.

[5] IMPACTA. State of the Art of Space Thermal Control Systems.

[6] Dupont, V., and Thome, J. R. Evaporation in microchannels: influence of the channel diameter on heat transfer. Microfluid Nanofluid, 1, 119–127. 2005.

[7] Dupont, V., Popper, C., Bertha, M., Hoffait, S., and de Ryckel, A. Experimental investigation of the effect of the vibration on the operation of the direct contact condensation “box” component of a Capillary Jet Loop. In Proceedings of the joint 22nd IHPC and 16th IHPS, Nakhon Pathom, Thailand, November 24-28. 2024

[8] Hecht, F. New development in FreeFem++. J. Numer. Math., 20, 251–265. Retrieved from https://freefem.org/.2012.

[9] Pedroza Torres, M., Hernandez Naranjo, J. A., Rioboo, R., Dupont, V., & Lemort, V. Figures of merit and their applicability for fluid selection in two-phase mechanically pumped loops based on 1D simulation results. In Proceedings of the 42nd UIT International Heat Transfer Conference. UIT. 2025.